Influence of Short-Period Variations of Atmospheric Forcing on Large-Scale Ocean Dynamics

Yu.D. Resnyanskii, A.A. Zelenko, V.N. Stepanov, and B.S. Strukov
Hydrometeorological Research Center of Russian Federation
Email: resny@mail.ru

Introduction

The variability of the ocean dynamics is controlled by both atmospheric forcings (AF) on its surface and its own internal dynamics. Due to the nonlinearity, dynamical processes in the ocean at different time scales interact with each other. Consequently, the structure and evolution of oceanographic fields, even at larger scales, also depend on the short-period variability of the AF, no matter how short.

Estimates of this dependence are obtained using the ocean general circulation model, which is part of the oceanographic data assimilation system of the Hydrometeorological Center of Russia.

Numerical experiments

These estimates were obtained by comparing the results of two numerical experiments carried out over the period 2001–2014 with atmospheric forcing DFS5.2 (DRAKKAR Forcing Sets, Dussin et al., 2016). The simulations started from initial state of rest with the January climatological temperatures and salinities from the WOA13 atlas. The experiments differed only in the time discreteness of the AF sets (air temperature and humidity at a height of 2 m, wind speed at a height of 10 m, downward fluxes of short-wave and long-wave radiations, and precipitation rate): 3–24 hours in the main experiment (further as E1 experiment) and 1 month in the experiment with the time- averaged AF (E2).

The ORCA1 configuration of the NEMO version 3.6 model (Madec, 2008) coupled to the LIM3 ice model (Rousset et al., 2015) was used for the numerical experiments. All model outputs in both experiments were stored as successive 5-day means throughout the whole integration period.

Results

Kinetic energy

The kinetic energy averaged over the World Ocean within the entire water column from the surface to the bottom, normalized to the density of water $KE = \overline{\frac{1}{2}(u^2 + v^2)}$ (u and v are the 5-day averages of the horizontal velocity components, the overbar denotes averaging over area and depth) in the E1 experiment was systematically higher by ~20% compared to E2. By the end of the fourth model year, a quasi-steady state has been reached with KE fluctuating between 5(4) and 6.5(5) cm^2s^{-2} for the E1 (E2) experiment that indicates a fast baroclinic adjustment of the velocity field to the initial density field, which subsequently has been slowly changed.

Atlantic meridional overturning circulation and meridional heat transport

The upper cell of the Atlantic meridional overturning circulation (AMOC) in almost the entire Atlantic in E1 turned out to be more intense than in E2, with maximum differences between E1 and E2 to the south of 20°N about of 2–5 Sv (1 Sv = $10^6 m^3/s$). Near-surface circulation cell driven by wind between 30°N and 60°N, in E1 it also turned out to be ~2 Sv more intense than in E2. The Deacon cell in E2 is about 15 Sv weaker than in E1.

The elimination of short-term variability of the AF led to a decrease in meridional heat transport (MHT) in the Atlantic Ocean from 35°S up to ~30°N by almost 30%. This decrease is mainly due to the weakening of the AMOC. The MHT weakened by ~15–20% to the north of 45°N due to a decrease of the contribution of the oceanic circulation gyre to E2. The exception is the region from ~37°N up to ~45°N (at the boundary of oceanic gyres), where the MHT value from E2 exceeded the value from E1, and the difference between the MHT values at ~40°N reached almost 40%.

Thermohaline fields

One of the most distinct consequences of the impact of short-period variations, noted in (Resnyanskii and Zelenko, 1999), is a change of the seasonal cycle of the surface water temperature. In our experiments, a decrease in the seasonal changes of the surface temperature due to short period variations was noted, as is seen from the map of amplitude differences between E1 and E2 (Fig. 1a). It was the most noticeable in moderate and high latitudes polewards of 40°N and 40°S. The magnitude of the decrease (~2°C) was almost quarter of the amplitude of seasonal cycle itself (~8°C). The reverse picture was observed in the subtropical latitudes ($|\varphi|$ = 20–40°) where the amplitude increased. The influence of the short-term AF variations on

seasonal changes in near-surface salinity in most areas was either weak or almost independent of the AF type (Fig. 1b).

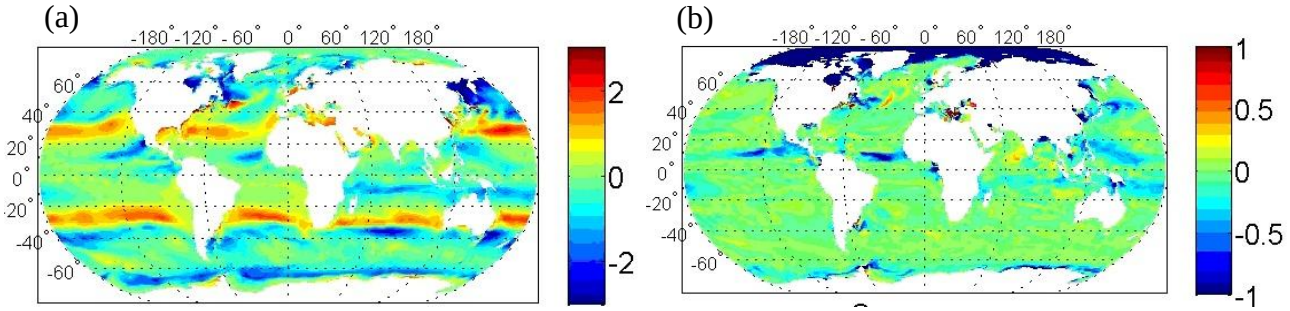

Fig. 1. Difference between amplitudes of seasonal changes in surface temperature (a) and salinity (b) in experiments E1 and E2. The amplitude is defined as 2009–2013 mean module of the difference between monthly averages in September and March.

From a comparison of the modelled temperature fields with the WOA13 data, the results of calculations in E1 are in better agreement with WOA13 than E2. Due to the stronger Ekman pumping in E1, the salinity in the area of subtropical ocean gyres turns out to be higher. The salinity field is slightly better reproduced in E2 up to ~45°N, however, to the north of 45°N, the model salinity field in E1 is closer to the observational data. Thus, considering the short-term variability of the AF allows to more accurately reproduce the temperature field in all areas of the World Ocean and the salinity field at high latitudes.

Sea Ice

In seasonal changes of the area occupied by sea ice, a significant difference between E1 and E2 in the Northern hemisphere was observed from June to September: the area occupied by sea ice in E2 exceeded the NOAA/NSIDC observed value in August, while in E1 this area was underestimated in August by about by 2×10^6 km^2. Both calculations overestimate the area occupied by sea ice, but the difference between the calculation results of E1 and the NOAA/NSIDC data was two times less than for E2.

A closer agreement between the results of the E1 experiment and NOAA/NSIDC data is also noted for calculations for the seasonal variability of sea ice volume. In the northern hemisphere, the monthly averaged volume of sea ice in E1/E2 (14.3×10^3/15.3×10^3 km^3) varies from a minimum of 4.1×10^3/7.8×10^3 km^3 in August-September to a maximum of 25.1×10^3/22.9×10^3 km^3 in April (according to PIOMAS data minimal and maximal values are 4.2×10^3 and 22.3×10^3 km^3, respectively). In the southern hemisphere, the monthly averaged volume of sea ice in E1/E2 reaches its maximum in October 18.9×10^3/17.5×10^3 km^3 and then decreases to 2.7×10^3/5.2×10^3 км^3 in February (according to GIOMAS data, the maximum value in September–October is 18.7×10^3 km^3, and minimum in February is 1.9×10^3 km^3).

Summary

The results of numerical experiments with the ORCA1/LIM3 model indicate that neglecting short-term variations in atmospheric forcings can significantly distort the large-scale characteristics of the ocean and sea ice reproduced by ocean-sea ice models and thereby affect the quality of forecasts with such models.

It is worth noting that the above presented results are obtained with the ocean circulation model with a relatively low (~1 deg) horizontal resolution, in which most of the mesoscale oceanic eddies are parametrized. These effects in high-resolution models can be even more pronounced.

References

Dussin R., Barnier B., Brodeau L., and Molines J.-M. (2016). The Making of the DRAKKAR Forcing Set DFS5. DRAKKAR/MyOcean Report 01-04-16. 34 p.

Madec G. and the NEMO team (2008). NEMO ocean engine. Note du Pôle de modélisation, Institut Pierre-Simon Laplace (IPSL), France, No 27. ISSN No 1288-1619, 386 pp.

Resnyanskii Yu.D.,and Zelenko A.A. (1999). Effects of Synoptic Variations of Atmospheric Forcing in an Ocean General Circulation Model: Direct and Indirect Manifestations. *Russian Meteorology and Hydrology*. **24**(9), 42–50.

Rousset C., Vancoppenolle M., Madec G. et al. (2015). The Louvain-La-Neuve sea ice model LIM3.6: Global and regional capabilities. *Geosci. Model Dev*., **8**, 2991–3005. https://doi.org/10.5194/gmd-8-2991-2015.